Electronic Supplementary Information

Densification of Cellulose Acetate-Derived Porous Carbons for Enhanced Volumetric Hydrogen Adsorption Performance

Hiroshi Matsutaka*[abc], Aya Kashifuku[ab], Takaaki Orii[a], Daigo Miyajima[ad], Naoki Uchiyama[abe], Satoshi Wada[b] and Hirotomo Nishihara[cf]

[a]*RIKEN Baton Zone Program, 2-1 Hirosawa, Wako 351-0198, Japan*
[b]*RIKEN Center for Advanced Photonics, 2-1 Hirosawa, Wako 351-0198, Japan*
[c]*Institute of Multidisciplinary Research for Advanced Materials, Tohoku University, 2-1-1 Katahira, Aoba-ku, Sendai 980-8577, Japan*
[d]*School of Science and Engineering, The Chinese University of Hong Kong, Shenzhen, 2001 Longxiang Boulevard, Longgang District, Shenzhen 518172, China*
[e]*Atsumitec Co., Ltd., 7111 Ubumi, Yuto-cho, Nishi-ku, Hamamatsu 431-0192, Japan*
[f]*Advanced Institute for Materials Research (WPI-AIMR), Tohoku University, 2-1-1 Katahira, Aoba-ku, Sendai 980-8577, Japan.*

*Corresponding Author: Hiroshi Matsutaka
E-mail: hiroshi.matsutaka@riken.jp

1. Experimental Section

1.1 Materials and reagents

Cellulose acetate (CA, acetylation degree: 55.3 %) and Cellulose triacetate (CTA, acetylation degree: 61.6 %) were purchased from Fujifilm Wako Pure Chemical Corporation, respectively. Potassium hydroxide (KOH), polyvinyl alcohol (PVA, polymerization degree of 2000), and hydrochloric acid (HCl) were purchased from Kanto Chemical Co. Polyvinylpyrrolidone (PVP, average molecular weight: 40000 (K30), and average molecular weight: 360000 (K90), respectively), hydroxypropyl cellulose (HPC) were purchased from Tokyo Chemical Industry Co. Polyethylene oxide (PEO), Zinc nitrate hexahydrate ($Zn(NO_3)_2 \cdot 6H_2O$, 98 %), and 2-methylimidazole (2MeIM, 99 %) were purchased from Sigma-Aldrich. All reagents and solvents were used without further purification.

1.2 Preparation of CA-derived carbon powder

(1) Synthesis of CA-based Char by hydrothermal method

CA powder (19.2 g) was dissolved in 60 mL of deionized water, then the mixture was transferred to a 100 mL Teflon-lined stainless-steel autoclave and heated to 250 ℃ for 1 hour. The resulting black solid was put into 500 mL of deionized water and stirred for approximately 3 h at room temperature. The black solid/water mixture was then filtered using a PTFE membrane (pore diameter 0.1 µm), washed with 200 mL of deionized water several times, and finally, the residue of black solid on the filter was transferred to a petri dish and dried at 100 ℃ overnight under vacuum. A dry black powder (hydrochar, Char) was obtained at 5.2 g (yield: approximately 27 wt%).

(2) KOH activation of the CA-based Char

The hydrothermal compound (180 mg, Char) and KOH powder (360 mg) were added to a container and mechanically mixed by ball milling using a bead crusher machine. The resulting mixture was carefully collected and placed in an alumina boat, and set into a quartz tube (inner diameter: 26 mm). The mixture was calcined at 700 °C for 2 h under a nitrogen flow atmosphere (N_2 flow rate: 0.1 L min^{-1}) with a heating rate of 3 ℃ min^{-1} using an electronic furnace. The obtained black solid was added to 300 mL of deionized water and stirred at room temperature for 3 h to remove KOH. Hydrochloric acid (HCl, 1 mol L^{-1}) was then added to neutralize the solution, followed by filtration. The sample on the filter was washed several times with 300 mL of deionized water under reduced pressure to completely remove any residual KOH and related products. The sample on the filter was collected and then placed in a petri dish and dried at 100 ℃ under vacuum overnight. The black powder was obtained at 70 mg (yield: approximately 11 wt%). Note that the yield of the activation treatment in step (2) from the Char is approximately 38 wt%. The activation conditions involve mixing Char and KOH in a Char/KOH ratio of 1/2 above. Here, in this study, the mixing ratio is also set at 1/0.3, 1/0.5, 1/1, 1/1.5, 1/3, and 1/4 (w/w). In addition, the following conditions are being changed and considered. The mixture was activated to a given temperature (600–800 °C) for a duration of 30 min to 12 h, with the N_2 gas flow rate varying from 0.06 L min^{-1} to 1.5 L min^{-1}, respectively.

1.3 Preparation of CA-derived carbon pellets

The CA carbon pellets were prepared as shown in Fig. S1. The preparation method is described as follows:

(1) Typically, approximately 6 mg of CA-derived carbon powder was placed into a 4 mm diameter cemented carbide die with a spacer (circled by a dotted line, Fig. S1). And then, 3 drops of a PVA aqueous solution (10 mg mL^{-1}), which was prepared by stirring PVA powder in deionized water vigorously and dissolved in advance, were added and put using an upper punch. The upper punch was pressurized to 10 kN (800 MPa applied pressure) at room temperature to pre-form the sample and then it was left to sit overnight.

(2) The die containing the sample was dried at 50 °C under vacuum for more than 4 hours to remove water. The die set was carefully removed from the oven, the spacer was taken out, and the sample set was pressed at the same pressure of 800 MPa again at 150 °C with a hot press and left to sit overnight.

(3) Heating was stopped, and then, after slowly cooling to room temperature, the mold was released from the die set to obtain a CA carbon pellet. The pellet mass was weighed using a balance. The thickness of the pellet was measured with a digital micrometer. The volume of the pellet was then calculated, and thus the bulk density was manually estimated.

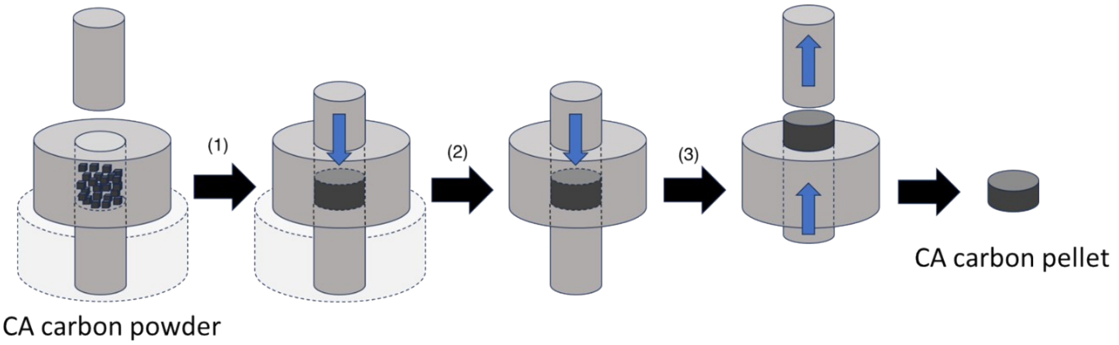

Fig. S1 Schematic illustration of the preparation of CA-derived porous carbon pellets from powers.

1.4 Preparation of MOF-derived carbon powder

(1) Synthesis of MOF (ZIF-8)

Typically, zeolitic imidazolate framework-8 (ZIF-8) was synthesized according to a previously reported procedure with slight modifications.[1,2] First, $Zn(NO_3)_2·6H_2O$ (180 g, 0.6 mol) was dissolved in 2 L of methanol, and 2MeIM (396 g, 4.8 mol) was separately dissolved in 2 L of methanol, respectively. The $Zn(NO_3)_2·6H_2O$ solution was poured into the 2MeIM solution under vigorous stirring in a 4-L conical flask. The mixture was agitated for 1 h at room temperature. Then, the white colloidal solution was sealed and kept overnight. After decanting the supernatant, the resultant milky liquid was centrifuged at 3500 rpm for 10 min to remove excess 2MeIM. Fresh methanol was added to the precipitate, mixed using a pipette, and centrifuged again. This process was repeated several times to thoroughly wash the sample. Finally, the resultant white solid was dried overnight under vacuum at 80 °C. The white powder was obtained at approximately 32 g (yield: 5.6 wt%).

(2) Synthesis of ZIF-8-derived carbon powder

The ZIF-8 powder (6.0 g) was placed in a boat and set into a quartz tube in the same procedure as mentioned above. The powder was calcined at 900 °C for 159 h under a N_2 flow atmosphere using an electronic furnace. The black powder was obtained at approximately 200 mg (carbonization yield: 3.3 wt%).

1.5 Preparation of ZIF-8-derived carbon pellets

ZIF-8-derived carbon pellets were prepared as shown in Fig. S2, which is the same procedure as the CA-derived carbon pellets mentioned above.

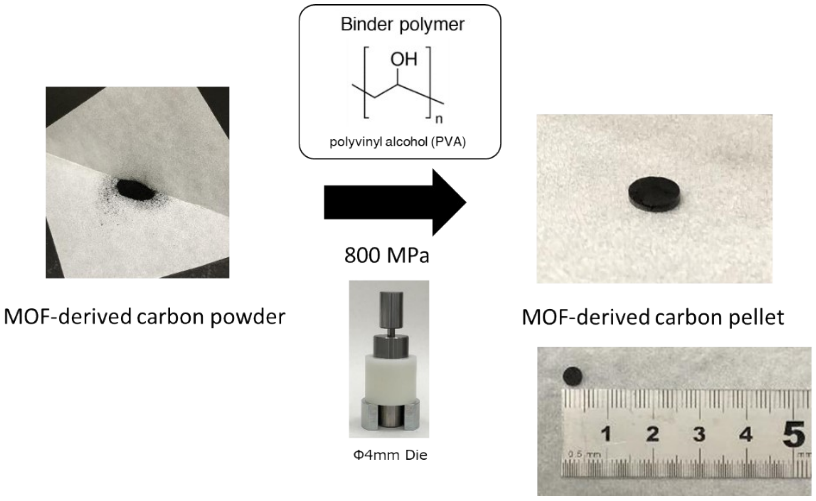

Fig. S2 Scheme for producing pellets from MOF (ZIF-8)-derived carbon powder. Photos show the ZIF-8 carbon before and after compaction at 800 MPa through die molding pelletization.

2. Characterization

Nitrogen sorption and hydrogen sorption were measured using a BELSORP-Max II instrument (MicrotracBEL, Japan) at -196 ℃ up to 1 bar, respectively. Carbon dioxide sorption isotherms were measured using the same instrument at 0 ℃ up to 1 bar. Before sorption measurements, a blank glass tube was heated at 300 ℃ for more than 1 h in a high vacuum (< 1 Pa) to remove all physisorbed species from the surface of the tube. The weight of the blank tube was measured as a reference for accurately measuring the net weight of the sample. The Brunauer-Emmett-Teller (BET) specific surface area (SSA) was calculated by using the data points on the adsorption isotherm in the range of relative pressure $P/P_0 = 0.05$–0.3. Pore size distribution was calculated by Quenched Solid Density Functional Theory (QSDFT) method (equilibrium kernel at -196 ℃, carbon slit-model) using the software package VersaWin (Anton Paar, Austria) for N_2 adsorption isotherms and Non-Local Density Functional Theory (NLDFT) method using the same analytical software for CO_2 adsorption isotherms. The total pore volume was calculated at $P/P_0 = 0.96$, based on the pore-filling pressures of micropores (pores smaller than 2 nm) and mesopores (2–50 nm), using the monolayer adsorption amount and the N_2 liquid-equivalent adsorption determined from BET plot results. Environmental scanning electron microscopy (SEM) images were obtained using an environmental scanning electron microscope with a 10–20-kV electron beam (Thermo Fisher Scientific, Quattro S).

3. Supplementary Figures and Tables

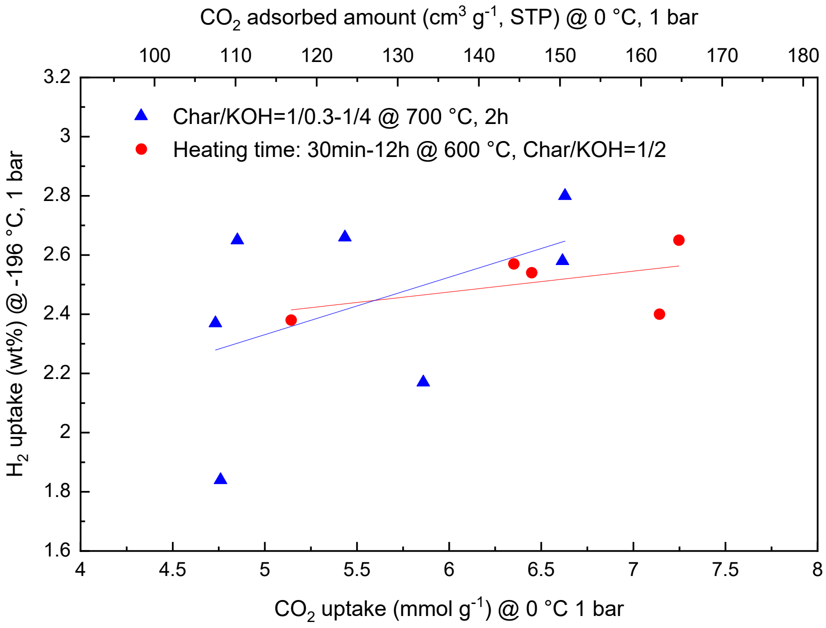

Fig. S3 Plot of the relationship between CO$_2$ adsorption at 0 °C and 1 bar and H$_2$ adsorption at -196 °C and 1 bar. The red circles represent CA-derived carbon powders with a fixed Char/KOH ratio of 1/2 at 600 °C, where the heating time varies. The blue triangles represent changes in the Char/KOH ratio when calcinated at 700 °C for 2 h under KOH activation. A straight line represents the approximate trend for each set of data (the coefficient of determination (R^2) for each line is as follows: red line, $R^2 = 0.265$, and blue line, $R^2 = 0.232$).

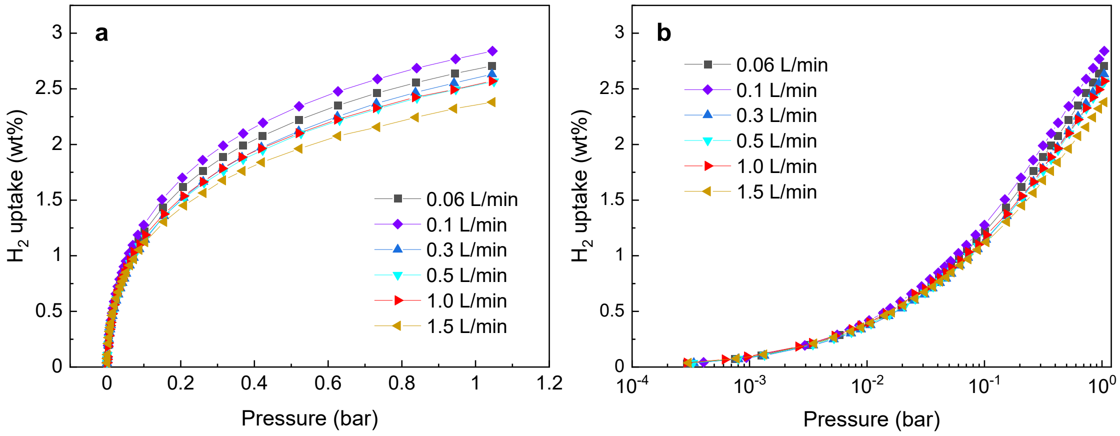

Fig. S4 Adsorption behavior of CA-derived carbon powders prepared with different KOH activation conditions, varied N_2 gas flow rate ranging from 0.06 to 1.5 L min^{-1}. (a) H_2 adsorption isotherms at -196 °C. (b) H_2 adsorption isotherms with the horizontal axis of (a) displayed logarithmically. Note that, the other activation conditions were fixed; the Char/KOH mixing ratio was set at 1/2, the activation temperature was fixed at 700 °C, and the heating time was fixed at 2 h.

Table S1 Adsorption characteristics of CA-derived carbon powders with varied N_2 gas flow rate during KOH activation, corresponding to Fig. 5 and Fig. S4.

N_2 flow rate [L min^{-1}]	S_{BET} ^{a} [m^2 g^{-1}]	V_{total} ^{b} [cm^3 g^{-1}]	Yield ^{c} [%]	H_2 uptake ^{d} [wt%]
0.06	1999	1.02 (0.85)	8.9	2.68
0.1	2013	1.01 (0.86)	10.6	2.80
0.3	2215	1.15 (0.93)	3.9	2.60
0.5	1980	1.04 (0.85)	5.3	2.53
1.0	1983	1.14 (0.85)	2.0	2.54
1.5	1827	0.98 (0.78)	3.9	2.35

[a] Gravimetric specific surface area calculated by the BET method from the N_2 adsorption isotherms at -196 °C in the range P/P_o=0.05-0.3. [b] Total pore volume calculated at P/P_o=0.96. The values in parentheses are cumulative micropore volumes calculated by the QSDFT method from the N_2 adsorption isotherms. [c] Calculated from the ratio of the final KOH-activated product mass to the raw material of CA. [d] Gravimetric H_2 storage density at -196 °C and 1 bar.

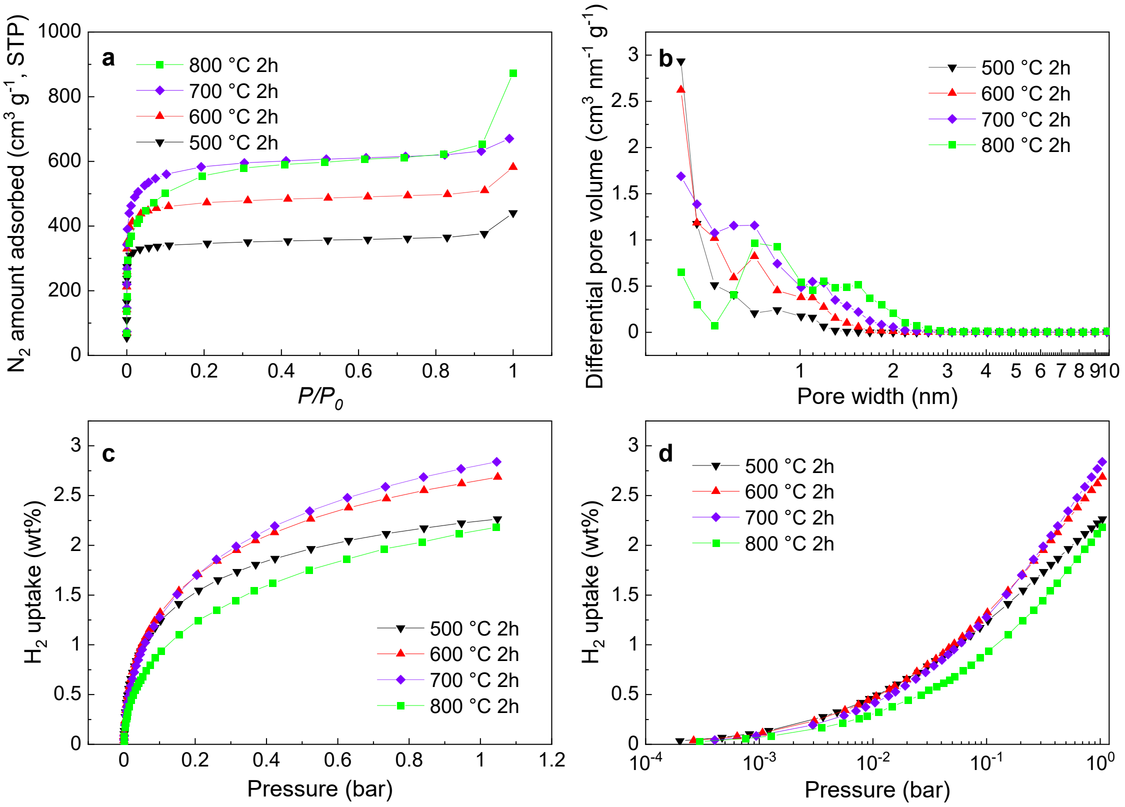

Fig. S5 Adsorption behaviors of cellulose-derived carbon powders activated by using KOH as activating reagent, varied activation temperature from 500 °C to 800 °C. (a) N_2 adsorption isotherms at -196 °C. (b) Pore size distribution calculated from N_2 adsorption isotherms in (a) using the QSDFT method. (c) H_2 adsorption isotherms at -196 °C. (d) H_2 adsorption isotherms with the horizontal axis of (c) displayed logarithmically. Note that, the other activation conditions were fixed; the Char/KOH mixing ratio was set at 1/2, the heating time was 2 h, and the N_2 gas flow rate was 0.1 L min^{-1}.

Table S2 Adsorption characteristics of CA-derived carbon powders with varied activation temperatures under KOH activation conditions.

Temperature [°C]	S_{BET} [a] [m^2 g^{-1}]	V_{total} [b] [cm^3 g^{-1}]	Yield [c] [%]	H_2 uptake [d] [wt%]
500	1144	0.63 (0.50)	14.6	2.25
600	1569	0.84 (0.58)	14.4	2.65
700	2013	1.01 (0.86)	10.6	2.80
800	1967	1.18 (0.81)	1.5	2.15

[a] Gravimetric specific surface area calculated by the BET method from the N_2 adsorption isotherms at -196 °C in the range P/P_o=0.05-0.3. [b] Total pore volume calculated at P/P_o=0.96. The values in

parentheses are cumulative micropore volumes calculated by the QSDFT method from the N_2 adsorption isotherms. [c] Calculated from the ratio of the final KOH-activated product mass to the raw material of CA. [d] Gravimetric H_2 storage density at -196 ℃ and 1 bar.

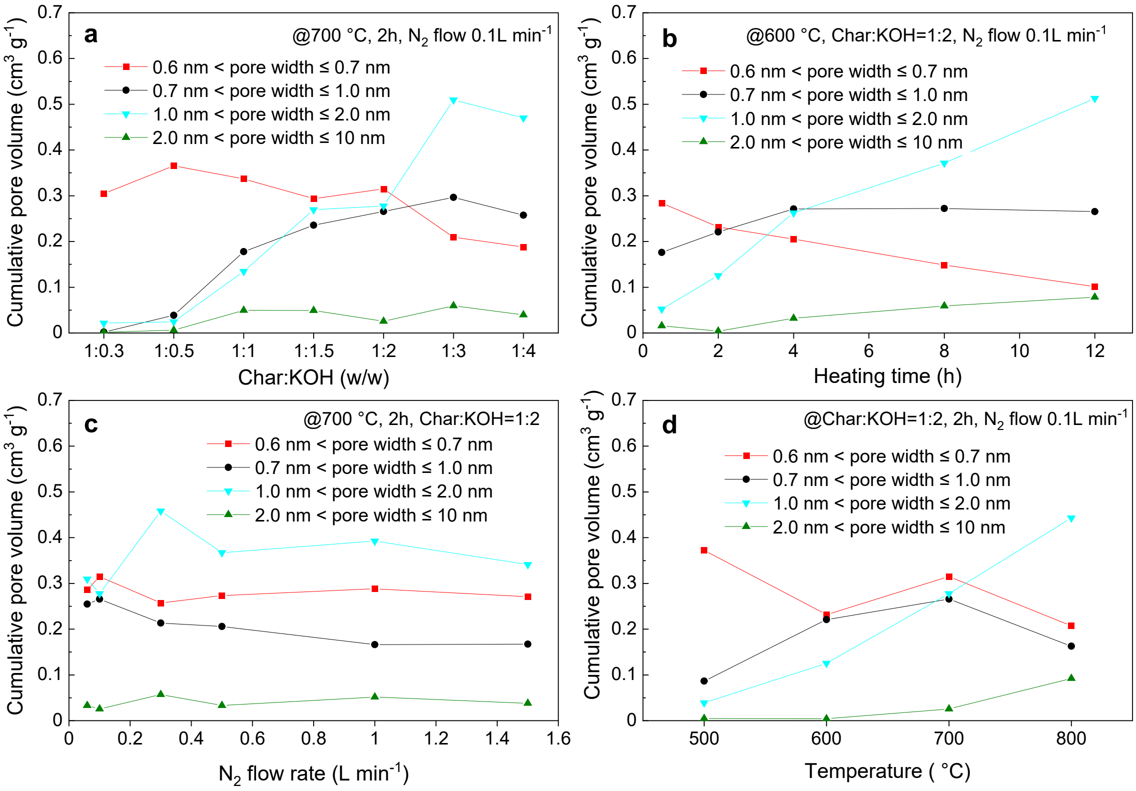

Fig. S6 Pore size section analysis based on pore size distribution data calculated using the QSDFT method from N_2 adsorption isotherms of the CA-derived carbon powers. Pore size sections are 0.6 nm, 0.7 nm, 1.0 nm, 2.0 nm, and 10 nm, respectively. Under the KOH activation conditions, (a) when Char/KOH is changed from 1/0.3 to 1/4, (b) when the heating duration is changed from 30 min to 12 h, (c) when the N_2 gas flow rate is changed from 0.06 to 1.5 L min^{-1}, and (d) when the activation temperature is changed from 500 ℃ to 800 ℃.

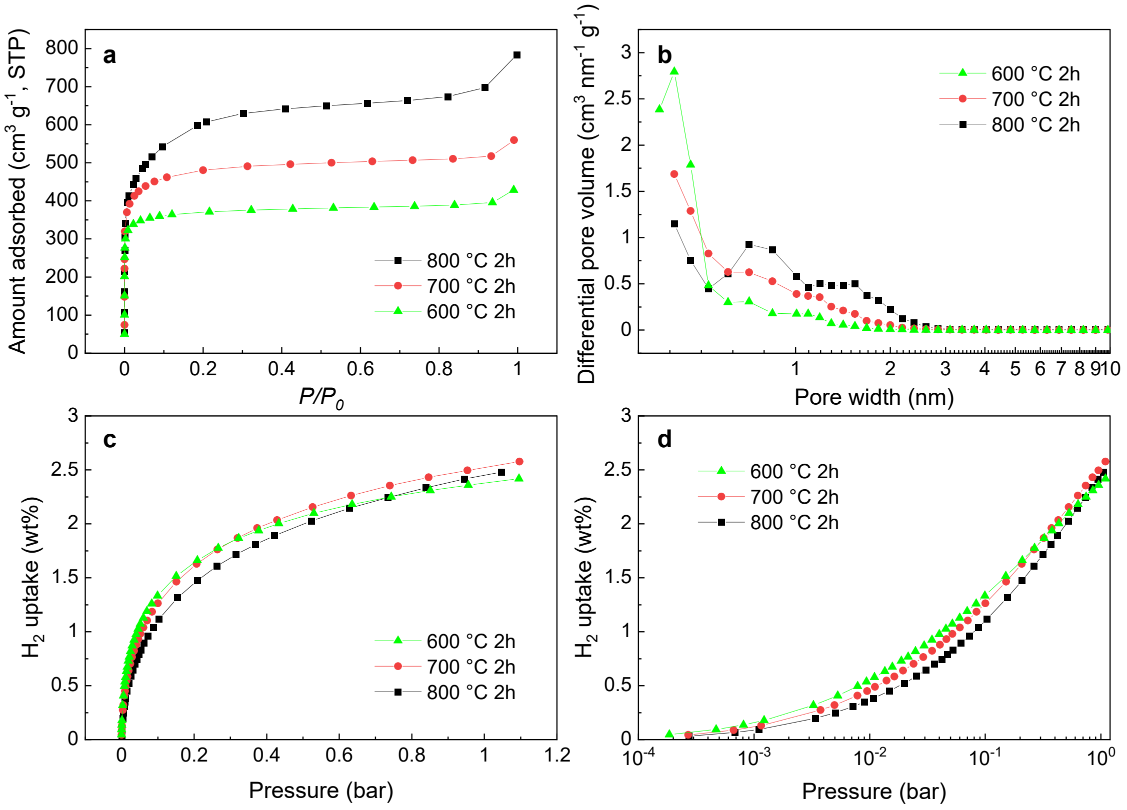

Fig. S7 Adsorption behaviors of cellulose-derived carbon powders activated by using K_2CO_3 as activating reagent instead of KOH, varied activation temperature from 600 ℃ to 800 ℃. (a) N_2 adsorption isotherms at -196 ℃. (b) Pore size distribution calculated from N_2 adsorption isotherms in (a) using the QSDFT method. (c) H_2 adsorption isotherms at -196 ℃. (d) H_2 adsorption isotherms with the horizontal axis of (c) displayed logarithmically. Note that, the other activation conditions were fixed; the Char/K_2CO_3 mixing ratio was set at 1/2, the heating time was 2 h, and the N_2 gas flow rate was 0.1 L min^{-1}, respectively.

Table S3 Adsorption characteristics of CA-derived carbon powders with varied activation temperatures under K_2CO_3 activation conditions.

Temperature [℃]	S_{BET} [a] [m^2 g^{-1}]	V_{total} [b] [cm^3 g^{-1}]	Yield [c] [%]	H_2 uptake [d] [wt%]
600	1235	0.63 (0.52)	14.3	2.38
700	1630	0.83 (0.57)	10.7	2.52
800	2115	1.15 (0.80)	4.2	2.45

[a] Gravimetric specific surface area calculated by the BET method from the N_2 adsorption isotherms at -196 ℃ in the range P/P_o=0.05-0.3. [b] Total pore volume calculated at P/P_o=0.96. The values in parentheses are cumulative micropore volumes calculated by the QSDFT method from the N_2

adsorption isotherms. [c] Calculated from the ratio of the final KOH-activated product mass to the raw material of CA. [d] Gravimetric H_2 storage density at -196 °C and 1 bar.

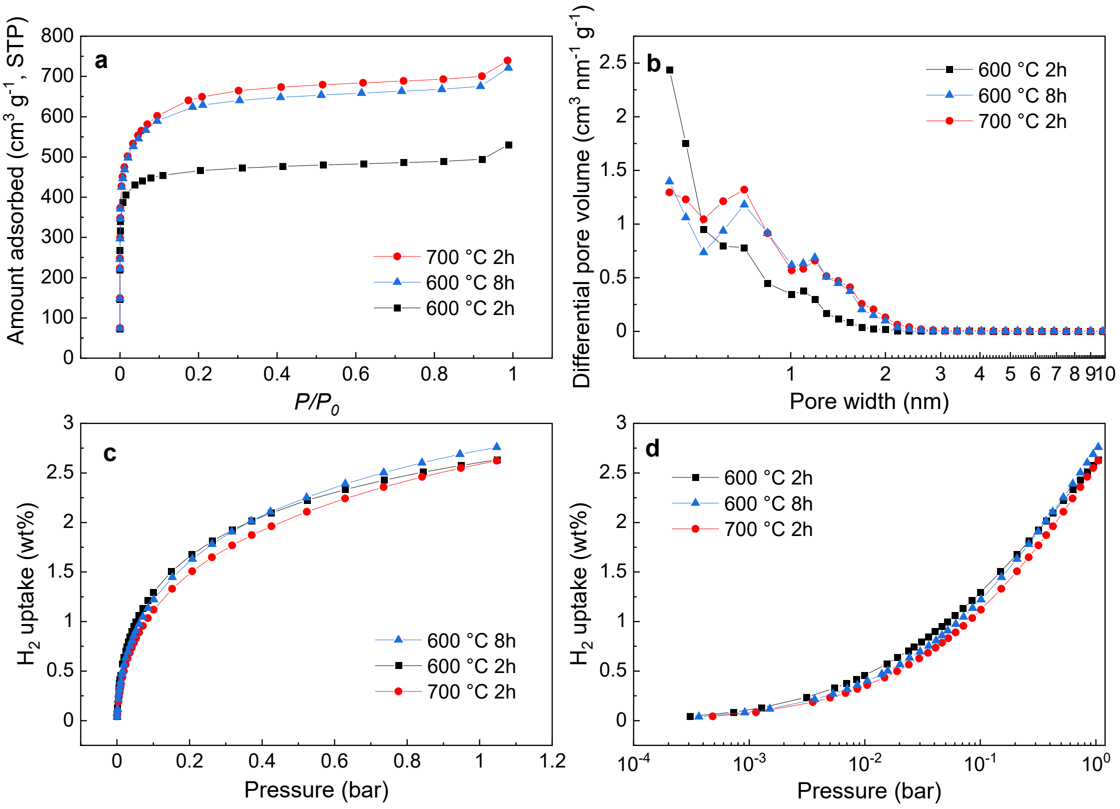

Fig. S8 Adsorption behaviors of cellulose triacetate (CTA)-derived carbon powders activated under different KOH activation conditions for the same CTA Char. (a) N_2 adsorption isotherms at -196 °C. (b) Pore size distribution calculated from N_2 adsorption isotherms in (a) using the QSDFT method. (c) H_2 adsorption isotherms at -196 °C. (d) H_2 adsorption isotherms with the horizontal axis of (c) displayed logarithmically. Note that, the CTA-derived Char was prepared under the same conditions as the CA Char sample, using a solvothermal process at 250 °C for 2 h. Other activation conditions were held constant; the Char/KOH mixing ratio was set at 1/2, and the N_2 gas flow rate was 0.1 L min^{-1}, respectively.

Table S4 Adsorption characteristics of CTA-derived carbon powders with varied activation temperatures and times under KOH activation conditions.

Temperature [°C]	Time [h]	S_{BET} [a] [m^2 g^{-1}]	V_{total} [b] [cm^3 g^{-1}]	Yield [c] [%]	H_2 uptake [d] [wt%]
600	2	1556	0.80 (0.68)	14.4	2.61
600	8	2144	1.09 (0.93)	8.4	2.72
700	2	2237	1.12 (0.95)	9.6	2.59

[a] Gravimetric specific surface area calculated by the BET method from the N_2 adsorption isotherms at -196 ℃ in the range P/P_o=0.05-0.3. [b] Total pore volume calculated at P/P_o=0.96. The values in parentheses are cumulative micropore volume calculated by the QSDFT method from the N_2 adsorption isotherms. [c] Calculated from the ratio of the final KOH-activated product mass to the raw material of CTA. [d] Gravimetric H_2 storage density at -196 ℃ and 1 bar.

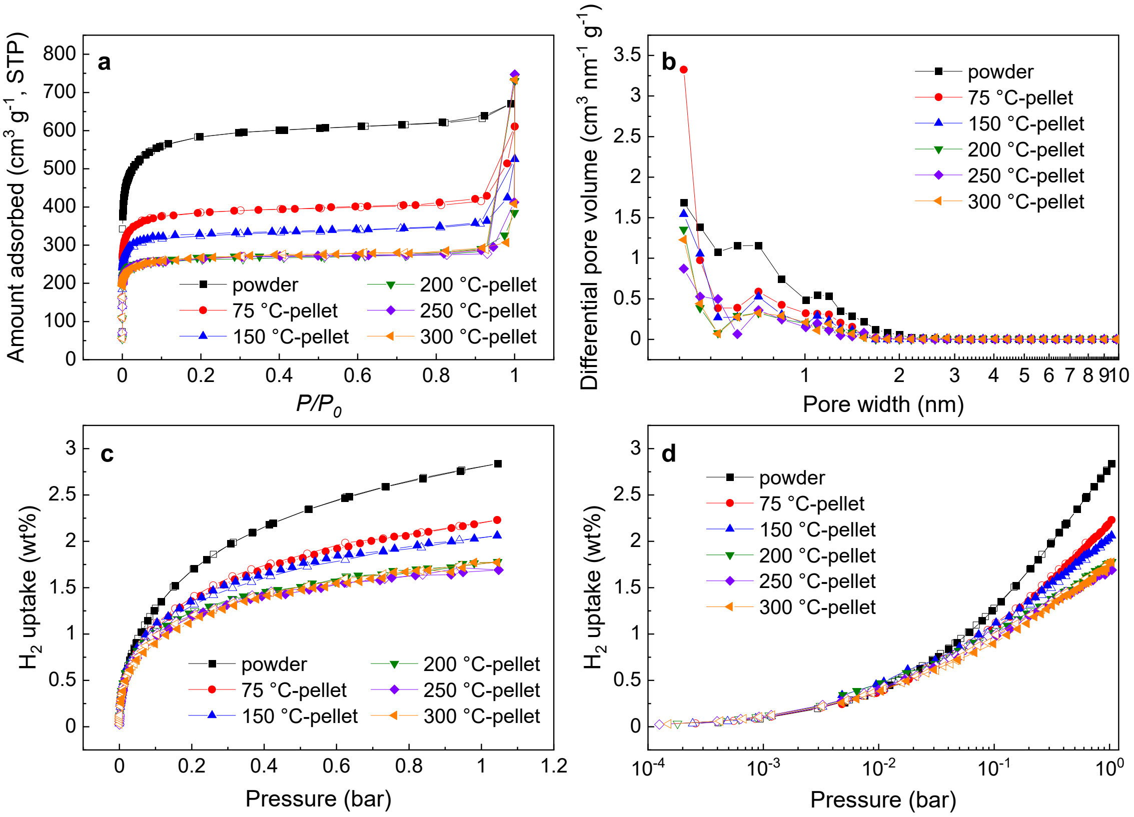

Fig. S9 Comparison of the adsorption behaviors of cellulose-derived carbon powder and its pellets prepared at various temperatures during the pelletizing process. (a) N_2 adsorption isotherms at -196 °C. (b) Pore size distribution calculated from N_2 adsorption isotherms in (a) using the QSDFT method. (c) H_2 adsorption isotherms at -196 °C. (d) H_2 adsorption isotherms with the horizontal axis of (c) displayed logarithmically. Note that the hollow color symbol indicates the adsorption side, while the filled color symbol represents the desorption side.

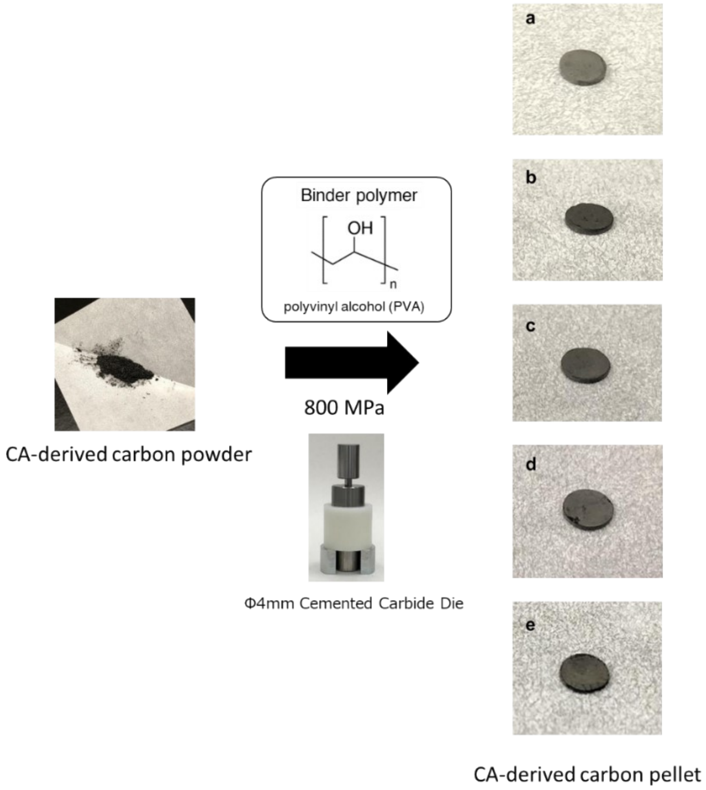

Fig. S10 Scheme for producing pellets from CA-derived carbon powder prepared at different temperatures during the pelletizing process. Photos show the CA carbon before and after compaction at a pressure of 800 MPa, using die molding at temperatures of (a) 75 ℃, (b) 150 ℃, (c) 200 ℃, (d) 250 ℃, and (e) 300 ℃, respectively.

Table S5 Adsorption properties of the CA-derived carbon powders and pellets.

No.	Sample [a]	Form [b]	Binder [c]	Bulk Density [g cm^{-3}]	BET SSA[d] [m^2 g^{-1}]	Vol. BET SSA [m^2 cm^{-3}]	Gravimetric H_2 uptake [wt%]	Volumetric H_2 uptake [g-H_2 L^{-1}]
1	CA batch 1	Powder	—	—	2312	—	2.55	—
2	CA batch 1	Pellet (75 °C)	PVA	0.69	1853 (-20%)	1251	2.34 (-8%)	16.0
3	CA batch 1	Pellet (150 °C)	PVA	0.80	1724 (-45%)	1091	2.53 (-1%)	20.3
4	CA batch 2	Powder	—	—	2013	—	2.80	—
5	CA batch 2	Pellet (75 °C)	PVA	0.85	1298 (-36%)	1104	2.20 (-21%)	18.7
6	CA batch 2	Pellet (150 °C)	PVA	0.97	1088 (-46%)	1051	2.04 (-27%)	19.8
7	CA batch 2	Pellet (200 °C)	PVA	0.95	878 (-56%)	830	1.76 (-37%)	16.7
8	CA batch 2	Pellet (250 °C)	PVA	1.10	883 (-56%)	972	1.70 (-39%)	18.7
9	CA batch 2	Pellet (300 °C)	PVA	0.96	891 (-56%)	858	1.76 (-37%)	17.0
10	CA batch 2	Pellet (75 °C)	PVA (5 mg/mL)	0.86	1266 (-37%)	1084	2.20 (-21%)	18.8
11	CA batch 2	Pellet (150 °C)	PVA (5 mg/mL)	0.74	1095 (-46%)	808	2.08 (-26%)	15.4
12	CA batch 2	Pellet (75 °C)	PVA (3 mg/mL)	—	—	—	—	—
13	CA batch 3*	Powder	—	—	2396		2.66	
14	CA batch 3*	Pellet (75 °C)	MC	0.69	1453 (-39%)	1000	2.16 (-19%)	14.9
15	CA batch 3*	Pellet (75 °C)	PVP (K90)	0.89	1236 (-48%)	1105	1.79 (-33%)	16.0

16	CA batch 3*	Pellet (75 °C)	PVP (K30)	0.82	1347 (-44%)	1102	2.10 (-21%)	17.2
17	CA batch 3*	Pellet (75 °C)	PEO	0.92	937 (-61%)	859	1.51 (-43%)	13.9
18	CA batch 3*	Pellet (75 °C)	HPC	0.72	1346 (-44%)	969	2.08 (-22%)	15.0
19	CA batch 4	Powder	—	—	2413	—	2.62	—
20	CA batch 5	Powder	—	—	1829	—	2.72	—
21	CA batch 6	Powder	—	—	1980	—	2.33	—

[a] The same batch number of CA-derived carbon is the same single lot that Char prepared through solvothermal synthesis, activated under the same conditions: Char/KOH = 1/2 (w/w), activation temperature = 700 °C, heating time = 2 h, and N_2 flow rate = 0.1 L min^{-1}. [b] The values in parentheses represent the temperature at which the mixture of carbon powder and PVA binder was pressed at a pressure of 800 MPa. Typically, a 75 °C or 150 °C press was conducted. [c] The parentheses in PVA represent the binder addition concentration during the preparation process. A small addition of PVA solution, like 3 mg/mL, was insufficient to produce pellets. The non-parenthetical PVA represents a PVA solution concentration of 10 mg/mL added, corresponding to approximately 10–15 wt% content in the pellets. The parentheses of PVP represent the product name for the different average molecular weights; K90 is 360000, and K30 is 40000, respectively. [d] The values in parentheses represent the percentage reductions after pelletizing the powder.

*The activation conditions for CA batch 3 powder are as follows: Char/KOH = 1/3 (w/w), activation temperature = 700 °C, heating time = 2 h, and N_2 flow rate = 0.1 L min^{-1}.

Table S6 Adsorption properties of the ZIF-8-derived carbon powder and the pellets.

No.	Sample	Form [a]	Binder	Bulk Density [g cm^{-3}]	BET SSA[b] [m^2 g^{-1}]	Vol. BET SSA [m^2 cm^{-3}]	Gravimetric H_2 uptake [b] [wt%]	Volumetric H_2 uptake [g-H_2 L^{-1}]
1	ZIF-8 carbon batch 1	Powder	—	—	3008	—	2.54	—
2	ZIF-8 carbon batch 1	Pellet (75 ℃)	PVA	0.54	2344 (-22%)	1255	2.13 (-16%)	11.4
3	ZIF-8 carbon batch 1	Pellet (150 ℃)	PVA	0.54	2051 (-32%)	1107	2.15 (-15%)	11.6
4	ZIF-8 carbon batch 1	Pellet (RT)	PVA	0.25	2633 (-12%)	645	2.20 (-13%)	5.4
5	ZIF-8 carbon batch 2	powder	—	—	1935	—	2.27	—
6	ZIF-8 carbon batch 2	Pellet (75 ℃)	PVA	0.41	1418 (-27%)	586	1.91 (-16%)	7.9
7	ZIF-8 carbon batch 2	Pellet (150 ℃)	PVA	0.55	1212 (-37%)	662	1.78 (-22%)	9.7

[a] The values in parentheses represent the temperature at which the mixture of ZIF-8 carbon powder and PVA binder was pressed in the die set at a pressure of 800 MPa. [b] The values in parentheses represent the percentage reductions after pelletizing to the powder. Note that both ZIF-8 carbon powders (batch 1 and batch 2) were prepared using the same method detailed in Experimental Section 1.4; however, the degree of carbonization differed, resulting in carbonization yields of 3.3% for batch 1 and 12.2% for batch 2, respectively.

Table S7 Micropore volume analysis of the CA-derived carbon and MOF-derived carbon for the powders and the pellets.

Sample	V_{total} [a] [cm^3 g^{-1}]	$V_{0.6\text{-}2.0\ nm}$ [b] [cm^3 g^{-1}]	$V_{0.6\text{-}1.0\ nm}$ [c] [cm^3 g^{-1}]	$V_{0.6\text{-}0.7\ nm}$ [d] [cm^3 g^{-1}]
ZIF-8 carbon powder	1.65	1.12	0.24	0.03
ZIF-8 carbon pellet	1.27 (-23%)	0.73 (-35%)	0.19 (-21%)	0.06
CA carbon powder	1.17	0.93	0.38	0.07
CA carbon pellet	0.96 (-18%)	0.60 (-36%)	0.30 (-21%)	0.14

[a] Total pore volume (V_{total}) calculated at P/P_o=0.96, based on the BET plots data. [b] Pore volume ($V_{0.6\text{-}2.0\ nm}$) is a cumulative pore volume within the range of 0.6 nm to 2.0 nm calculated by the QSDFT method. [c] Pore volume ($V_{0.6\text{-}1.0\ nm}$) is a cumulative pore volume within the range of 0.6 nm to 1.0 nm calculated by the QSDFT method. [d] Pore volume ($V_{0.6\text{-}0.7\ nm}$) is a cumulative pore volume within the range of 0.6 nm to 0.7 nm calculated by the QSDFT method. Note that the values in parentheses represent percentage reductions after pelletizing to its powder.

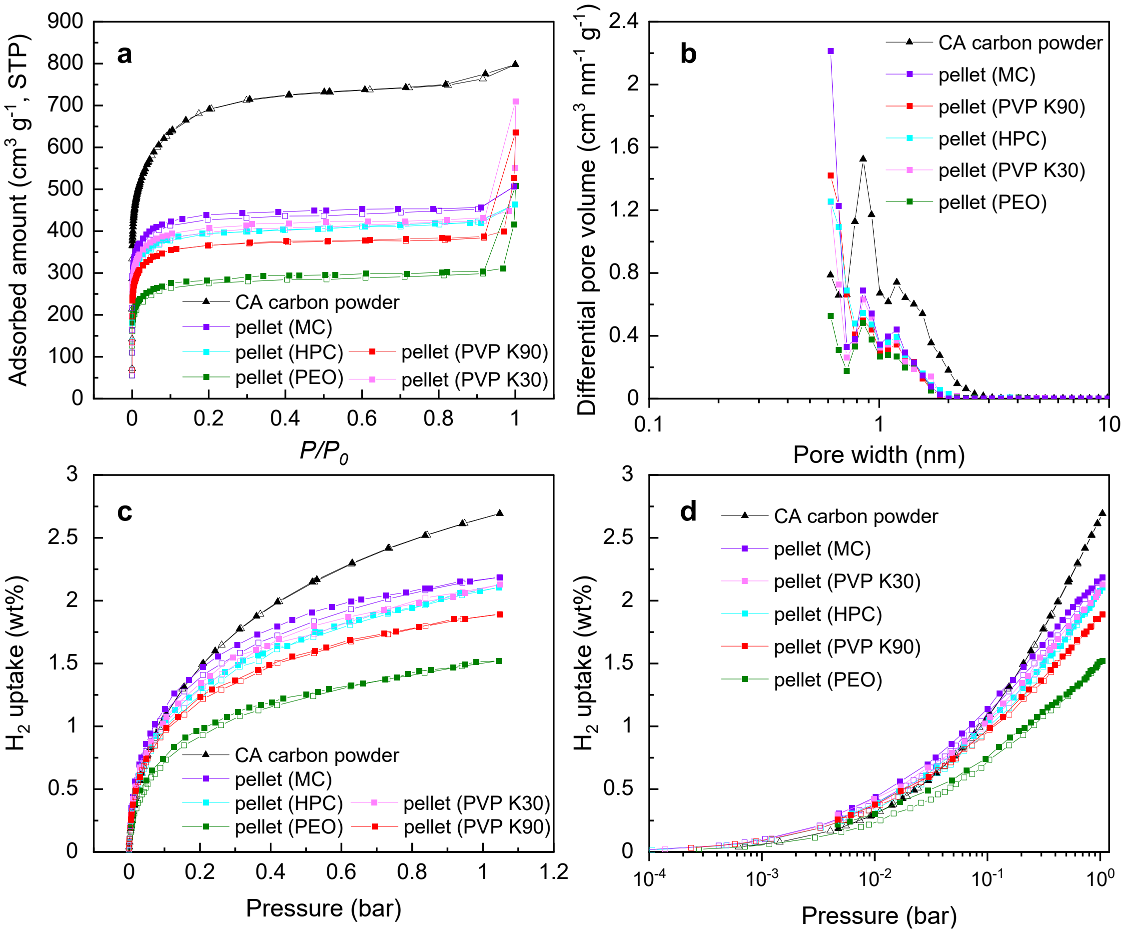

Fig. S11 Comparison of the CA carbon pellets with different kinds of binder polymers. (a) N_2 adsorption-desorption isotherms at -196 ℃. (b) Pore size distribution of the CA-derived carbon powder and the pellets with different binders, calculated from the N_2 adsorption isotherms of (a) using the QSDFT method. (c) H_2 adsorption isotherms at -196 °C. (d) H_2 adsorption isotherms with the horizontal axis of (c) displayed logarithmically. Note that, the CA carbon powder comes from CA batch 3 in Table S4. Pellet (MC) refers to a CA carbon pellet with an MC binder, which was produced by pelletizing the CA carbon powder. Pellet (PVP K90) refers to a CA carbon pellet with a PVP binder (Mw 360,000). A pellet (HPC) refers to a CA carbon pellet with an HPC binder. Pellet (PVP K30) refers to a CA carbon pellet with a PVP binder (Mw 40,000). A pellet (PEO) refers to a CA carbon pellet with a PEO binder. Note that the hollow color symbol indicates the adsorption side, while the filled color symbol represents the desorption side.

Table S8 Comparison of volumetric hydrogen storage capacity with other reported MOF pellets (monoliths) and porous carbon pellets.

Pellet	Binder	Conditions	Volumetric H_2 uptake [g-H_2 L^{-1}]	Ref.
SNU-70	—	5 bar, -196 ℃	9.0*	[3][6]
ZTC/rGO	rGO	5 bar, -196 ℃	22.4*	[3][4]
ZTC	—	20 bar, -196 ℃	38	[5]
MOF-5/ENG	ENG	5 bar, -196 ℃	12.9*	[3][7]
MIL-101(Cr)	—	80 bar, -196 ℃	40*	[6]
MOF-5	—	5 bar, -196 ℃	16.5*	[3][7]
MOF-177	—	5 bar, -196 ℃ (~60 bar, -196 ℃)	13.1* (25.8)	[3][8]
UiO-66	—	100 bar, -196 ℃	39	[9]
UiO-66/PIM-1	—	5 bar, -196 ℃	23*	[10]
HKUST-1	—	1 bar, -196 ℃	15.3*	[11]
ACM-2	WSC	40 bar, -196 ℃	29.7	[12]
ZIF-8 carbon	PVA	1 bar, -196 ℃	11.6	This work
CA carbon	PVA	1 bar, -196 ℃	20.3	This work

*Total hydrogen storage capacity, determined from measured excess H_2 uptake and the hydrogen quantity of gas-accessible volume at -196 ℃. Ref.[3] is based on calculated data.

4. Supplementary References

1. H. L. Jiang, B. Liu, Y. Q. Lan, K. Kuratani, T. Akita, H. Shioyama, F. Zong and Q. Xu, *J. Am. Chem. Soc.*, 2011, **133**, 11854–11857.
2. J. Cravillon, S. Münzer, S.-J. Lohmeier, A. Feldhoff, K. Huber and M. Wiebcke, *Chem. Mater.*, 2009, **21**,1410–1412.
3. S. S. Samantaray, S. T. Putnam and N. P. Stadie, *Inorganics*, 2021, **9**, 45.
4. A. Gabe, M. Ouzzine, E. E. Taylor, N. P. Stadie, N. Uchiyama, T. Kanai, Y. Nishina, H. Tanaka, Z.-Z. Pan, T. Kyotani and H. Nishihara, *J. Mater. Chem. A*, 2021, **9**, 7503–7507.
5. N. Balahmar, A. M. Lowbridge and R. Mokaya, J. Mater. Chem. A, 2016, 4, 14254–14266.
6. J. Purewal, M. Veenstra, D. Tamburello, A. Ahmed, A. J. Matzger, A. G. Wong-Foy, S. Seth, Y. Liu and D. J. Siegel, *Int. J. Hydrogen Energy*, 2019, **44**, 15135–15145.
7. J. Purewal, D. Liu, A. Sudik, M. Veenstra, J. Yang, S. Maurer, U. Müller and D. J. Siegel, *J. Phys. Chem. C*, 2012, **116**, 20199–20212.
8. R. Zacharia, D. Cossement, L. Lafi and R. Chahine, *J. Mater. Chem.*, 2010, **20**, 2145–2151.
9. S. E. Bambalaza, H. W. Langmi, R. Mokaya, N. M. Musyoka, J. Ren and L. E. Khotseng, *J. Mater. Chem. A*, 2018, **6**, 23569–23577.
10. S. E. Bambalaza, H. W. Langmi, R. Mokaya, N. M. Musyoka and L. E. Khotseng, I*nt. J. Hydrogen Energy*, 2021, **46**, 8607–8620.
11. D. G. Madden,D. O'Nolan, N. Rampal, R. Babu, C. Çamur, A. N. A. Shakhs, S.-Y. Zhang, G. A. Rance, J. Perez, N. P. M. Casati, C. Cuadrado-Collados, D. O'Sullivan, N. P. Rice, T. Gennett, P. Parilla, S. Shulda, K. E. Hurst, V. Stavila, M. D. Allendorf, J. Silvestre-Albero, A. C. Forse, N. R. Champness, K. W. Chapman and D. Fairen-Jimenez, *J. Am. Chem. Soc.*, 2022, **144**, 13729–13739.
12. M. Jordá-Beneyto, D. Lozano-Castelló, F. Suárez-García, D. Cazorla-Amorós and Á. Linares-Solano, *Microporous Mesoporous Mater*., 2008, **112**, 235–242.